Advances in three-dimensional coronary imaging and computational fluid dynamics: is virtual fractional flow reserve more than just a pretty picture?

Eric K.W. Poon[a], Umair Hayat[b], Vikas Thondapu[a,b], Andrew S.H. Ooi[a], Muhammad Asrar Ul Haq[b], Stephen Moore[c], Nicolas Foin[d], Shengxian Tu[e], Cheng Chin[a], Jason P. Monty[a], Ivan Marusic[a] and Peter Barlis[a,b]

Percutaneous coronary intervention (PCI) has shown a high success rate in the treatment of coronary artery disease. The decision to perform PCI often relies on the cardiologist's visual interpretation of coronary lesions during angiography. This has inherent limitations, particularly due to the low resolution and two-dimensional nature of angiography. State-of-the-art modalities such as three-dimensional quantitative coronary angiography, optical coherence tomography and invasive fractional flow reserve (FFR) may improve clinicians' understanding of both the anatomical and physiological importance of coronary lesions. While invasive FFR is the gold standard technique for assessment of the haemodynamic significance of coronary lesions, recent studies have explored a surrogate for FFR derived solely from three-dimensional reconstruction of the invasive angiogram, and therefore eliminating need for a pressure wire. Utilizing advanced computational fluid dynamics research, this virtual fractional flow reserve (vFFR) has demonstrated reasonable correlation with invasive measurements and remains an intense area of ongoing study. However, at present, several limitations and computational fluid dynamic assumptions may preclude vFFR from widespread clinical use. This review demonstrates the tight integration of advanced three-dimensional imaging techniques and vFFR in assessing coronary artery disease, reviews the advantages and disadvantages of such techniques and attempts to provide a glimpse of how such advances may benefit future clinical decision-making during PCI. *Coron Artery Dis* 26: e43–e54 Copyright © 2015 Wolters Kluwer Health, Inc. All rights reserved.

Introduction

Coronary artery disease (CAD) represents a significant health burden with the key pathological process being atherosclerosis. The invasive assessment of CAD relies upon catheter-based coronary angiography, and despite its limitations, it has remained the gold standard since its introduction over 30 years ago [1]. Quantitative coronary angiography (QCA) is based on the automated or semi-automated border detection of the contrast-filled lumen, and has become both the reference standard in research studies and provides objective assessment of diameter stenosis in clinical practice [1]. Angiography, however, provides a two-dimensional (2D) representation of the coronary arteries and lacks sufficient resolution to provide comprehensive lesion-level information. More recently, intravascular imaging has been complemented by optical coherence tomography (OCT), which, because of its superior resolution, provides detailed knowledge of the nature of the atherosclerosis process and also helps guide percutaneous coronary intervention (PCI) more accurately than angiography alone [2–4]. In addition,

physiological lesion assessment has been enhanced by the use of pressure wires measuring the fractional flow reserve (FFR) to help guide the need for PCI. This review provides an update on the latest developments in three-dimensional (3D) coronary imaging, discusses how such advances can be integrated into the assessment of haemodynamic significance of a lesion, and postulates their future roles in the catheterization laboratory.

Quantitative coronary angiography

Coronary angiography is the gold standard invasive imaging modality to diagnose CAD, and visual estimation of stenosis severity has been the traditional method to guide intervention [5]. This approach has several limitations highlighted in older studies conducted over a decade ago [6,7]. Interobserver and intraobserver assessment of angiographic disease severity varies from 15 to 45% as reported in numerous studies [8–10]. Advances in angiographic data processing have resulted in the ability to computationally reconstruct the coronary artery of interest in 2D or 3D [11] and to quantitatively analyse the

severity of lesions, a process known as QCA. Nallamothu *et al.* [12] more recently demonstrated once again that despite technological refinements in angiographic acquisition and processing, visual estimation of the degree of stenosis remains imprecise. In their study of 216 treated lesions, they found the mean difference in per cent diameter stenosis (%DS) between clinical interpretation and QCA to be $8.2 \pm 8.4\%$ reflecting higher %DS, on average, by clinical interpretation ($P < 0.001$). Of all the treated lesions graded as more than 70%DS by visual interpretation, approximately one-quarter were less than 70% by QCA [12]. These discrepancies may translate to inconsistencies in clinical decision-making in the catheterization laboratory [13]. QCA adds to the objectivity of angiographic evaluation and has been shown to improve the interobserver and intraobserver agreement [14,15]. It is a widely adapted benchmark tool in clinical trials and is recommended in clinical practice.

In QCA, coronary stenoses are assessed based on their geometric features. The minimum lumen diameter (MLD), reference vessel diameter and the %DS are some of the commonly used parameters to gauge stenosis severity [16]. Foley *et al.* [16] challenged the long held popularity of %DS among clinicians and proposed that absolute luminal measurements, especially MLD, should be the preferred parameter. The authors [16] performed quantitative analysis on 110 angiograms obtained immediately after angioplasty and on a repeat angiogram 24 h later. There was no difference in mean MLD or cross-sectional area between the immediate postangioplasty and 24-h postangioplasty period; however, reference vessel diameter increased significantly (presumably secondary to greater vasodilatory effect of the same dose of intracoronary nitrate at 24 h); therefore, %DS was also found to increase significantly [16]. This study highlighted that %DS, a widely utilized parameter, was subject to considerable variation as it relies upon the dimensions of normally appearing reference vessel. Whereas this was an intriguing finding, %DS continues to be used in contemporary research and clinical practice.

Does three-dimensional quantitative coronary angiography add extra value?
Whereas angiography provides excellent delineation of the arterial lumen and 2D-QCA adds to the objective assessment of the severity of DS, it is widely known that a 2D imaging profile of a 3D structure inherently carries certain limitations such as inadequate visualization of eccentric plaques, inaccurate estimation of disease severity in D-shaped or elliptical lumens and lack of spatial information as we know that vessels do not always have circular geometries [17]. Whereas some of these problems can be partly overcome by acquisition of multiple projections of coronary vasculature from a range of angles and creating a 3D 'approximation' of the diseased segment, 3D-QCA was developed to address some of

these limitations. Dvir *et al.* [18] analysed 38 angiographic images side by side using both 2D-QCA and 3D-QCA and reported a weak correlation for %DS calculation between the two methods ($r^2 = 0.94$ for MLD and reference diameter, $r^2 = 0.33$ for %DS; $P < 0.05$). They concluded that the assumption of circular cross-section is the main reason for the weaker correlation in %DS between 2D-QCA and 3D-QCA. Their findings were again confirmed by Bourantas *et al.* [19], who showed stronger correlation between 3D-QCA and intravascular ultrasound (IVUS) in lumen dimensions ($r = 0.8$) than 2D assessed %DS ($r = 0.34$). Ultimately, the greatest advantage of 3D-QCA may be that it offers improved assessment of the absolute lumen dimensions including length, diameter, tortuosity, and optimal views [20,21] and not just %DS.

Whereas QCA is a widely accepted reference technique in scientific research and catheterization laboratories, the fundamental limitations of %DS and loss in MLD cut-off criteria have been well documented [16]. It is important to remember that QCA is an anatomical tool, and %DS and MLD do not always confer physiologic significance of a coronary stenosis.

Optical coherence tomography
OCT, by virtue of its exceptionally high resolution (10–15 μm), is far superior to IVUS in delineating the intima–lumen border with excellent reproducibility [4, 22,23]. This fact generates a plausible hypothesis that OCT could have an expanded role in predicting the functional significance of a given stenosis. Previous IVUS studies have found that minimal lumen area (MLA) less than 4 mm^2 or less than 3 mm^2 were useful thresholds to indicate haemodynamically significant lesions when tested against an FFR value of less than 0.75 as reference standard [24,25], whereas a later IVUS study with much larger sample size brought the IVUS-MLA threshold down to 2.4 mm^2 when tested against an FFR value of 0.80 or less [26].

Correlation of OCT-measured luminal parameters and invasive FFR has been tested for intermediate severity coronary stenosis (Table 1). Gonzalo *et al.* [27] examined 61 stenoses of intermediate angiographic severity from 56 patients. Quantitative OCT-based measurements were evaluated against FFR threshold of 0.80 or less. The authors reported an overall moderate diagnostic efficiency of OCT with optimal cut-off value for MLA being less than 1.95 mm^2 [27]. Forty-seven of these patients also underwent IVUS and a comparison of results in participants with simultaneous OCT and IVUS evaluation did not show significant difference in diagnostic efficiency. The only exception was in a subgroup of smaller vessels (< 3 mm) in which OCT performed better [27].

Table 1 Correlation of optical coherence tomography-measured luminal parameters and invasive fractional flow reserve

	References		
	Gonzalo et al. [27]	Shiono et al. [28]	Zafar et al. [29]
Number of patients	56	62	30
Number of stenoses	61	59	41
FFR reference	≤ 0.80	< 0.75	≤ 0.80
Results			
AUC (95% confidence interval for MLA)	0.74 (0.61–0.84)	0.90 (0.82–0.97)	0.80 (0.64–0.91)
OCT MLD cut-off (mm)	< 1.34	< 1.35	< 1.23
OCT MLA cut-off (mm^2)	< 1.95	< 1.91	< 1.62
OCT reference lumen area (mm^2)	6.47 ± 2.72	6.30 ± 1.72	7.35 ± 3.21
Sensitivity for MLA (%)	82	93.5	70
Specificity for MLA (%)	63	77.4	97
Overall diagnostic sensitivity to predict functional stenosis severity	Moderate	Moderate	Moderate

AUC, area under the curve; FFR, fractional flow reserve; MLA, minimal lumen area; MLD, minimal lumen diameter; OCT, optical coherence tomography.

More recently, Zafar et al. [29] evaluated 41 stenoses from 30 patients with QCA, FFR and OCT. Using an FFR cut-off value of 0.80 or less, the authors concluded that the overall diagnostic efficiency of OCT-derived MLD and MLA to predict haemodynamic significance was moderate [29]. In further subgroup analysis, they also found that the MLA had high diagnostic efficiency in vessels with reference diameters less than 3 mm [29]. Optimum cut-off values for MLA and MLD in this study were found to be less than 1.62 and less than 1.23 mm^2, respectively [29]. The threshold of OCT luminal dimensions in this study are much lower compared with those reported by Gonzalo and colleagues (< 1.95 and < 1.34 mm^2) and other investigators who described MLA and MLD of less than 1.91 mm^2 and less than 1.35 mm^2, respectively [28]. Two major differences in Zafar et al.'s [29] study were that they chose an FFR threshold of less than 0.75 and used a time-domain OCT system that required imaging through an occlusive technique, which could have led to underestimation of luminal dimensions as the distal coronary perfusion pressure drops during balloon occlusion (Table 1) [28,29].

An important point to note is the difference in the range of reported MLA thresholds between IVUS and OCT studies, which in part is due to superior resolution of the OCT permitting accurate lumen definitions and partly due to the difference in the reference vessel size (5.5–11.9 mm^2 in IVUS studies and 6–7 mm^2 in OCT studies). It is also postulated that the IVUS catheter, due to its larger diameter (3 Fr, 1.0 mm) compared with the OCT wire (0.016 inches, 0.41 mm), can stretch smaller vessels (Dotter effect) [30]. Therefore, the combination of MLA and per cent area stenosis may provide more incremental information than the MLA alone.

At best, the correlation between OCT-derived anatomical measurements in predicting haemodynamic significance of an intermediate severity lesion remains modest. Although the studies discussed have shown higher sensitivity in smaller diameter vessels (< 3 mm), overall low specificity means that the exact role of OCT in this setting is yet to be established. Ultimately, it may have higher potential in ruling out ischaemia than ruling in.

Invasive fractional flow reserve
Fractional flow reserve-guided percutaneous coronary intervention versus quantitative coronary angiography-guided percutaneous coronary intervention
FFR is the current gold standard to determine haemodynamic significance of intermediate severity coronary stenosis [31–34] as demonstrated by multiple clinical studies [35–39]. In the DEFER trial [36], 181 out of 325 patients who had an FFR value of more than 0.75 were randomly stratified into performed-PCI versus deferred-PCI groups. Over a 5-year follow-up period, the deferred-PCI group had a lower incidence of major adverse cardiac events as compared with the QCA-guided PCI group (3.3 vs. 7.9%; P = 0.21). The DEFER trial not only demonstrated benefit of FFR-guided PCI using a cut-off value 0.75 or less but it also highlighted the discrepancy between FFR and QCA [40].

The Fractional Flow Reserve Versus Angiography for Multivessel Evaluation (FAME) trial [35] was a large, randomized multicentre study evaluating the advantage of FFR-guided PCI over angiography-guided PCI. A total of 1005 patients with more than 50%DS in more than two epicardial coronary arteries were recruited. The FAME trial utilized a higher cut-off FFR value of 0.80 or less to include patients within the uncertainty region (0.75 ≤ FFR ≤ 0.80) as multiple studies have shown that there is an increased risk of ischaemia within these FFR values [41,42]. FFR value of 0.80 or less has since become the clinical cut-off value most often used [43]. Nevertheless, there were substantially fewer decisions to proceed with PCI in the FFR-guided than the angiography-guided groups (1.9 ± 1.3 vs. 2.7 ± 1.2; P < 0.001). There were also fewer occurrences of major adverse cardiac events in FFR-guided PCI patients at 1-year follow-up (13.2 vs. 18.3%; P = 0.02) and at 2-year follow-up (17.9 vs. 22.4%; P = 0.08). The FAME trial not only demonstrated the benefit of FFR-guided PCI but also showed that FFR-guided PCI is more cost-effective [44]. By reducing the number of stents deployed and minimizing revascularization and other adverse clinical events, FFR-guided PCI saved ~ $2400/patient at 1-year follow-up [45]. Besides the FAME trial, several other studies involving more than 10 000 patients [37–39] have also reported better clinical outcomes using FFR guidance. These results [35,37–39] have led to class IA and IIA recommendations from the European Society of Cardiology [46] and the American College of Cardiology [47], respectively. One of the potentially major

limitations of FFR, however, is the inability to achieve maximum hyperaemia in patients with diffuse epicardial or microvascular disease, resulting in underestimation of lesion severity [34,45,48].

Effects of coronary flow reserve on fractional flow reserve measurements

Coronary flow reserve (CFR) can either be an invasive or noninvasive flow measurement used to quantify the increase in volumetric flow in coronary arteries during hyperaemia relative to baseline flow [49]. Unlike FFR, which has a universal maximum value of 1, there is theoretically no maximum CFR value. The optimum cut-off value for a haemodynamically significant lesion is also less well-defined in the literature. Published CFR cut-off values range widely from 1.7 to 2.5 for epicardial coronary arteries [50–54], limiting the use of CFR in clinical practice.

According to Young *et al.* [55] the pressure difference (ΔP) across an epicardial artery is related to the volumetric flow (Q) with the following fluid dynamic equation [56,57]:

$$\Delta P = AQ + BQ^2, \tag{1}$$

where A and B are constants that depend on the cross-sectional area of the stenosed and normal artery, the length of the stenosis and the rheology of human blood [55]. As a result, it is instinctive to believe that FFR is correlated to CFR. Di Mario *et al.* [58] studied 21 patients, reporting $r = 0.58$ ($P < 0.01$), demonstrating a weak correlation between FFR and invasive CFR. In addition, their study showed that patients with an FFR value of 0.75 or less usually have a CFR value of 2.0 or less. Another trial by Meimoun *et al.* [59] involving 50

patients reported a similar result ($r = 0.59$; $P < 0.01$) with noninvasively measured CFR. This study also raised a fundamental concern over correlating FFR and CFR values when drawing conclusions about myocardial ischaemia. In contrast to the study by Di Mario *et al.* [58], Meimoun *et al.* [59] showed that four patients with FFR value of 0.80 or less had a CFR value of more than 2.0 and two patients with FFR value of more than 0.80 showed CFR value of 2.0 or less, representing 12% of the patients in this study. A more recent retrospective cohort study [60] with 438 FFR and invasive CFR measurements showed that even though FFR is correlated to CFR ($r = 0.34$; $P < 0.001$), almost 40% of lesions show discordance between FFR and CFR.

Johnson *et al.* [60] demonstrated that neither invasive nor noninvasive CFR measurement techniques can be attributed to the discordance of FFR and CFR. Nonetheless, there remain numerous questions regarding the use of FFR and CFR in clinical practice. Gould *et al.* [61] argued that while FFR is the current gold standard to reflect the physiological significance of the lesions, it does not truly reveal ischaemic flow conditions in the same manner as CFR. In contrast, it has been observed that CFR varies with time [62,63]. Despite continuous adenosine infusion, saturation of the vascular smooth muscle receptor (A_{2A}), cAMP precursor exhaustion, or K_{ATP} channel simulation momentarily hyperpolarises vascular smooth muscle, potentially resulting in hyperaemic flow returning back to the baseline before it rises again [64]. Furthermore, because CFR can cover a wide range of values for different patients [65], it is inherently difficult to identify whether maximum hyperaemia has been achieved, an important prerequisite for FFR [60,66].

Table 2   Correlation of quantitative coronary angiography-based virtual fractional flow reserve to invasive fractional flow reserve

	References		
	Morris *et al.* [70]	Tu *et al.* [11]	Papafaklis *et al.* [71]
Number of patients	19	68	120
Number of vessels	22	77	139
% DS	–	46.6 ± 7.3	38.8 ± 10.9
Bifurcation lesions	1/22 (4.5%)	50/77 (64.9%)	–
Method			
3D artery models	Rotational angiography	Conventional angiography	Conventional angiography
Boundary conditions	Generic conditions for the whole cohort	Hyperaemic VFR and mean catheter pressure applied at inlet	Generic conditions, no other patient-specific data
Computational time	24 h (pulsatile)	< 10 min	15 min
Hyperaemia simulation	No	VFR from TIMI frame count; CFR = hyperaemic VFR/baseline VFR	Specified blood flow rates at inlet (1 and 3 ml/s)
FFR reference	≤ 0.80	≤ 0.80	< 0.82 (vFAI)
Results			
Correlation (*r*)	0.84	0.81	0.78
Diagnostic accuracy (%)	97	88	88
Sensitivity (%)	86	78	90
Specificity (%)	100	93	86
PPV (%)	100	82	79
NPV (%)	97	91	93

3D, three-dimensional; %DS, per cent diameter stenosis; CFR, coronary flow reserve; FFR, fractional flow reserve; NPV, negative predictive value; PPV, positive predictive value; TIMI, thrombolysis in myocardial infarction; vFAI, virtual functional assessment index; VFR, volumetric flow rate.

Virtual fractional flow reserve

Despite the established evidence that FFR has clinical and economic benefits, it remains an underutilized tool in interventional practice. Potential barriers may include the additional procedure time required, need for adenosine administration, as well as additional cost. Studies of noninvasive coronary computed tomographic angiography (CTCA)-based virtual fractional flow reserve (vFFR) in DISCOVER-FLOW [67], DeFACTO [68] and HeartFlowNXT [69] were able to obtain vFFR values within a reasonable amount of time (~5 h) with good accuracy, specificity and high negative predictive values using sophisticated lump parameter boundary conditions based on averaged populations.

vFFR is a method to determine the ischaemic potential of coronary stenoses from routine coronary angiography through application of computational fluid dynamics (CFD) simulations. vFFR has the potential to avoid the need for costly pressure catheters and the possible risks associated with cannulation of stenoses. There has been a great deal of interest in this field recently and some very promising work (Table 2) has been published in the medical literature.

Morris *et al.* [70] studied 19 patients with stable CAD in the VIRTU-1 study. They constructed the 3D coronary anatomy off-line using invasive rotational coronary angiography and applied generic boundary conditions in their CFD studies. vFFR was computed in 24 h/case with a high accuracy, sensitivity, specificity of 97, 86 and 100%, respectively, on a study population with relatively simple lesions [70]. Furthermore, the vFFR and invasive FFR were closely correlated ($r = 0.84$), showing that FFR may be reliably predicted without the need for hyperaemia induction.

Tu *et al.* [11] assessed the diagnostic performance of vFFR using invasive FFR as the reference standard in 77 vessels from 68 patients by constructing 3D-QCA models from standard angiographic projections taken 25° or more apart. Volumetric flow rates at hyperaemia were calculated from thrombolysis in myocardial infarction frame counts. They reported that vFFR, or the so-called FFR_{QCA}, correlated well with FFR ($r = 0.81$; $P < 0.001$) on a study population with homogeneous intermediate lesions. The overall accuracy of FFR_{QCA} for the diagnosis of ischaemia defined by FFR value of 0.80 or less was 88%, with positive and negative predictive values of 82 and 91%, respectively. One of the major advancements in this study was extremely fast computational time with the entire analysis taking less than 10 min. However, 3D reconstructions of the coronary arteries remain an interactive process, and substantial automation should be implemented to enable high-volume use.

Papafaklis *et al.* [71] recently published the results of 139 vessels (120 patients) with mild and intermediate lesions. By deriving a quadratic equation for the pressure difference (ΔP) across the lesions from the CFD results at blood flow rates (Q) of 1 and 3 ml/s, a ΔP–Q curve was constructed and the corresponding vFFR values were obtained. The area under the vFFR–Q curve [virtual functional assessment index (vFAI)] for Q 4 ml/s or less was calculated and the authors reported that diagnostic accuracy, sensitivity and specificity for the optimal vFAI cut-off point (≤ 0.82) were 88, 90 and 86%, respectively. They also reported a significant correlation between the vFAI and vFFR ($r = 0.78$; $P < 0.0001$).
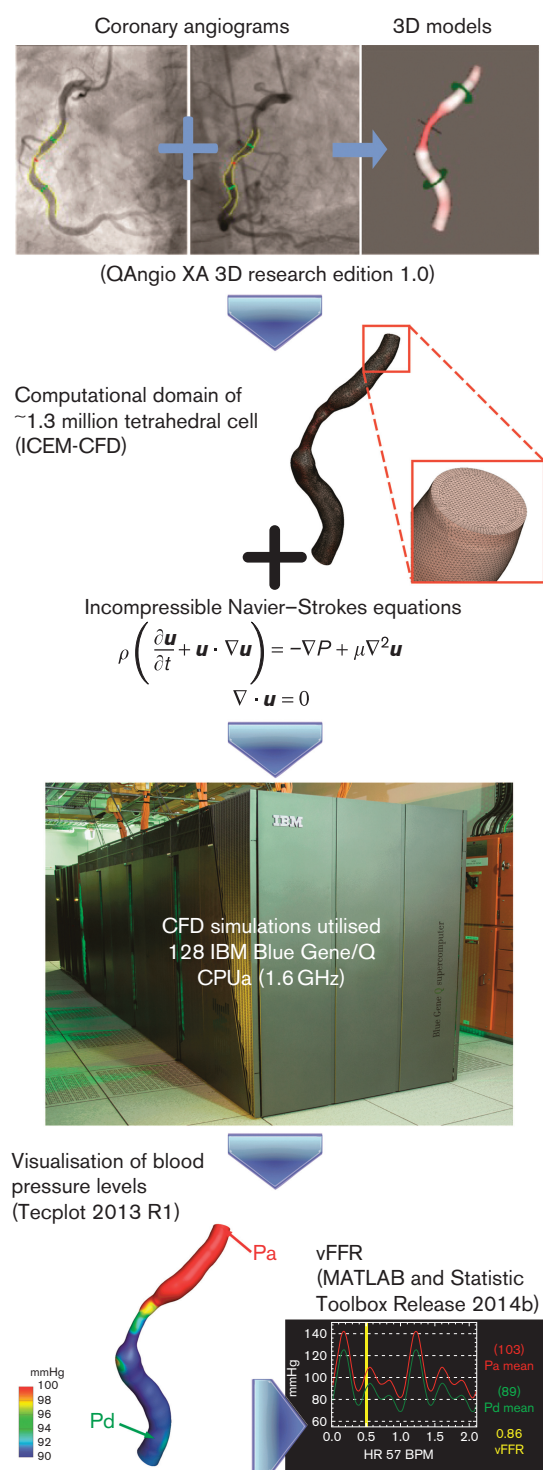
It is important to note that, apart from methodological differences in 3D reconstruction and CFD simulations in these three studies, the distribution of the severity of lesions included in the study population will also affect the diagnostic accuracy of these methods. That is, the inclusion of milder lesions will improve the detection metrics relative to higher degrees of stenosis.

Present computational fluid dynamics methodology and our experience

To examine the feasibility, utility and methodological strengths and weaknesses of vFFR, we studied 10 patients with intermediate angiographic stenoses. All patients had invasive FFR measurement at hyperaemia achieved with intravenous administration of adenosine. Invasive FFR served as the reference standard. The clinical cut-off value of 0.80 or less was used in accordance with established guidelines [41–43]. Patients with angina or non-ST-elevation myocardial infarction were included. Angiograms with minimum overlap or foreshortening of the artery of interest and in which the location of the distal pressure sensor was available were selected. Patients with prior transmural infarcts in the interrogated vessel territory, vessel protected by grafts and those with significant collaterals were excluded as these factors would have confounded the estimation of CFR and hyperaemic equations. Ostial and bifurcation lesions were also excluded for this pilot analysis.

Figure 1 shows the overview of the vFFR analyses using CFD methodology. We used QAngio XA 3D research edition 1.0 (Medis Special BV, Leiden, the Netherlands) to construct 3D models of coronary arteries from two angiographic projections acquired 25° or more apart. We selected eight left anterior descending arteries (LADs) and two right coronary arteries (RCAs). 3D models of coronary arteries were converted into STL files. We generated computational domains using ICEM-CFD (ANSYS Inc., Canonsburg, Pennsylvania, USA) from the 3D models of the coronary arteries. Each computational domain consists of ~1.3 million tetrahedral cells. The haemodynamics (i.e. blood velocity and pressure) in these coronary arteries were computed by directly solving the incompressible Navier–Stokes equations using a finite-volume solver OpenFOAM (OpenCFD Ltd, ESI group, Bracknell, UK). Time-dependent parabolic velocity profiles with mean baseline and hyperaemic velocity

Fig. 1

Coronary angiograms   3D models

(QAngio XA 3D research edition 1.0)

Computational domain of
~1.3 million tetrahedral cell
(ICEM-CFD)

Incompressible Navier–Strokes equations

$$\rho\left(\frac{\partial \boldsymbol{u}}{\partial t}+\boldsymbol{u}\cdot\nabla\boldsymbol{u}\right)=-\nabla P+\mu\nabla^2\boldsymbol{u}$$

$$\nabla\cdot\boldsymbol{u}=0$$

CFD simulations utilised
128 IBM Blue Gene/Q
CPUa (1.6 GHz)

Visualisation of blood
pressure levels
(Tecplot 2013 R1)

Pa

vFFR
(MATLAB and Statistic
Toolbox Release 2014b)

Pd

mmHg
100
98
96
94
92
90

140
120
100
80
60

mmHg

(103)
Pa mean

(89)
Pd mean

0.0 0.5 1.0 1.5 2.0
HR 57 BPM

0.86
vFFR

Flow chart of the vFFR analysis. BPM, beats per min; 3D, three-dimensional; CFD, computational fluid dynamics; HR, heart rate; Pa, aortic pressure; Pd, distal pressure; vFFR, virtual fractional flow reserve.

at 40 and 60 cm/s, respectively, were prescribed at the inlet to mimic pulsatile blood flow behaviour over a cardiac cycle. Generic waveforms [72] for the LAD and

RCA were used. The lumen wall was considered rigid and no-slip. A three-element Windkessel model with nonspecific vasculature resistance was used at the distal ends of the coronary arteries.

To ensure fast turnaround time, CFD simulations were performed using high-performance supercomputers at the Victorian Life Sciences Computational Initiative (Fig. 1). Each CFD study utilized 128 IBM Blue Gene/Q CPUs at 1.6 GHz. In-silico aortic pressure (Pa) was taken at the proximal end of the computational domain, whereas distal pressure (Pd) was monitored at the same location where the actual invasive FFR was taken during angiography. vFFR was calculated from the time-averaged values of Pa and Pd over one cardiac cycle. Results were presented using MATLAB and Statistic Toolbox Release 2014b (MathWorks Inc., Natick, Massachusetts, USA) and Tecplot360 2013R1 (Tecplot Inc., Bellevue, Wisconsin, USA). The diagnostic performance of vFFR was assessed against the invasive FFR results.

Figure 2 shows a representation of the vFFR analyses in RCA and LAD at simulated maximum hyperaemia. Blood pressure levels along these arteries are reported. The comparisons of each individual FFR and vFFR for all 10 cases are reported in Table 3. Our initial results reflect the inherent difficulties in vFFR methodology and highlight several issues facing the application of vFFR in the clinical setting. These variations in numerical setup have been shown to significantly alter the accuracy and speed of vFFR calculations and are discussed below.

One-for-all boundary conditions

One of the major limitations of the present CFD models is the use of generic boundary conditions. Similar to the CFD studies VIRTU-1 [70] and Papafaklis *et al.* [71], the present study incorporated generic flow velocities for both baseline (40 cm/s) and hyperaemia (60 cm/s) analyses. Depending on the proximal end diameter of the 3D model, this may result in a large variation in mean blood flow (ml/min) into the considered artery, therefore occasionally producing an unrealistic pressure difference and incorrect vFFR. In addition, specifying flow into the artery may neglect the effect of microcirculatory coronary flow [71]. The effect of generic boundary conditions was also reflected in our vFFR analyses in which three of the vFFR results were substantially lower than the invasive FFR results. These three cases suggest that this generic flow velocity (60 cm/s) cannot be applied to every patient. However, it remains unclear which lesion characteristics and in which individuals tailored-specific boundary conditions will be necessary. Other CFD studies such as DISCOVER-FLOW [67], DeFACTO [68] and HeartFlowNXT [69] trials used lump parameter boundary conditions to mimic the distal vascular tree resistance. These lump parameter boundary conditions may have overestimated the hyperaemic flow conditions [73].

Fig. 2
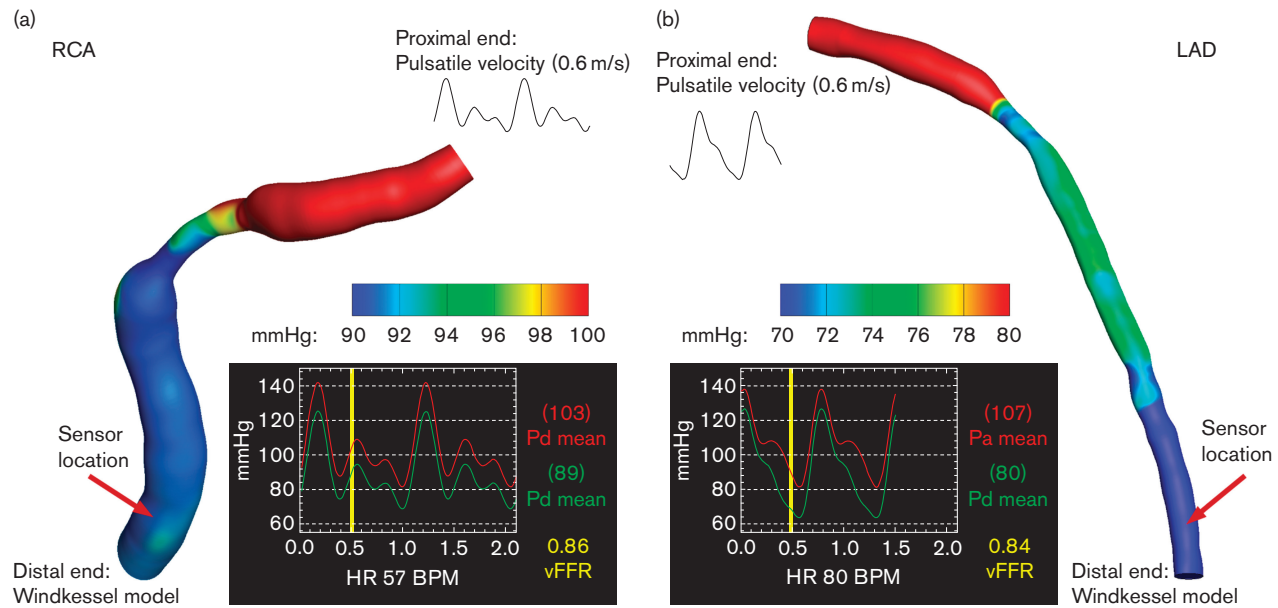
Graphical representations of virtual fractional flow reserve (vFFR) (cases 3 and 9). Blood pressure levels across the stenosis are represented by the colour contours of mmHg. Distal pressure (Pd) was measured at the pressure sensor location identified from coronary angiography during invasive fractional flow reserve (FFR) (red arrows). Aortic pressure (Pa) was obtained at the proximal end of the artery. Pulsatile blood flow velocity was implemented at the proximal end of the artery and a three-element Windkessel model mimics the vasculatures resistance at the distal end. (a) Case 3 is a right coronary artery (RCA) with a per cent diameter stenosis (%DS) = 55 diagnosed by quantitative coronary angiography and invasive FFR = 0.81, vFFR = 0.86. (b) Case 9 represents a left anterior descending artery (LAD) with a %DS = 45 and invasive FFR = 0.83, vFFR = 0.84. BPM, beats per min; HR, heart rate.

Table 3 Invasive and virtual fractional flow reserve values in 10 cases

Cases	Age	Vessel	%DS	Invasive FFR	vFFR
1	80	LAD	55	0.80	0.79
2	66	RCA	54	0.84	0.89
3	78	RCA	55	0.81	0.86
4	49	LAD	50	0.78	0.77
5	65	LAD	46	0.73	0.79
6	70	LAD	59	0.83	0.52
7	70	LAD	50	0.69	0.18
8	85	LAD	60	0.88	0.56
9	70	LAD	45	0.83	0.84
10	83	LAD	52	0.69	0.67

%DS, per cent diameter stenosis; FFR, fractional flow reserve; LAD, left anterior descending artery; RCA, right coronary artery; vFFR, virtual fractional flow reserve.

Segmented length of the three-dimensional models of coronary artery and pressure sensor location in computational fluid dynamics analyses

Additional factors that influence Pd are the segmented length of the 3D models of coronary arteries and the exact pressure sensor location, as the difference between proximal and distal pressure is a function of the distance between the two points (and other variables) according to Poiseuille's law. In addition, the two-step decrease in blood pressure level as illustrated in Fig. 2b elucidates the influence of the pressure sensor location on the vFFR analyses, especially in vessels in which serial lesions cannot be visually detected on angiography. Nevertheless, there is no universal agreement on the segmented length of 3D models, pressure sensor location and vFFR analyses. Further investigation is necessary to completely understand their roles in the vFFR analyses.

Spatial resolutions and geometrical assumptions on three-dimensional reconstruction of coronary arteries using coronary computed tomographic angiography and coronary angiography

The numerical accuracy, sensitivity and specificity of vFFR is also greatly affected by the limited spatial resolution of CTCA and coronary angiography [74]. In fact, whereas CTCA-based vFFR provides an innovative noninvasive FFR diagnosis technique, the anatomical variation of the coronary arteries should not be ignored when there is a substantial separation period between CTCA and invasive FFR [75]. Time-varying anatomical changes may alter the correlation between invasive FFR and CTCA-based vFFR. The disparity of results between the DISCOVERY-FLOW and DeFACTO trials was also shown to be closely related to the small variation in image processing protocol and was addressed in HeartFlowNXT [69]. Although coronary angiography may provide a better spatial resolution than CTCA [70], coronary arteries are often assumed to have circular/elliptical cross-section contour during reconstruction. The effects of artificially smoothing the coronary arteries on vFFR remain unclear [76]. Ultimately, the accuracy of

any CFD-based method relies on the resolution of the source image.

## Lengthy computational fluid dynamics studies

The final hurdle to the utilization of vFFR as an online tool in daily clinical use is the enormous time and computational resources that are required to carry out a single vFFR study. On average, our vFFR CFD studies need a total of 26 h, from imaging processing to data analysis, on a single case. Generally speaking, pulsatile flow CFD studies of coronary arteries will require 5–24 h analysing time on a super computer [70,73]. This is a substantial amount of time before clinicians can make any decision as compared with an invasive FFR procedure. This long computational time can be significantly reduced by partially solving the incompressible Navier–Stokes equations. More specifically, by neglecting the time-derivative term ($\partial u/\partial t$) in the incompressible Navier–Stokes equations, a converged flow solution and data analysis can be obtained with 10 min of time using 16 Intel(R) Xeon(R) CPUs E5645 at 2.40 GHz. Similar vFFR analysis time for steady flow simulations was also reported by Tu *et al.* [11] and Papafaklis *et al.* [71]. Figure 3 presents a comparison between steady flow simulations and pulsatile flow simulations (CFD run time 10 min vs. 25 h). In brief, vFFR can be predicted reasonably well with steady flow simulations. However, steady flow simulation is unable to predict the time-to-time variation of the pressure difference during a cardiac cycle (see inset in Fig. 3b). A pulsatile flow simulation can potentially provide improved information to clinicians such as instantaneous wave-free ratio [77], turbulent flow and variations in wall shear stress [78] that not only help determine the haemodynamic significance of a lesion but also potentially predict the long-term effect of the lesion on coronary flow in the artery. Finally, the presence of turbulent flow can substantially alter distal pressure, which is not considered with steady flow simulations. The impact of turbulent flow on vFFR results cannot be underestimated as stenoses often lead to highly turbulent flow [79].

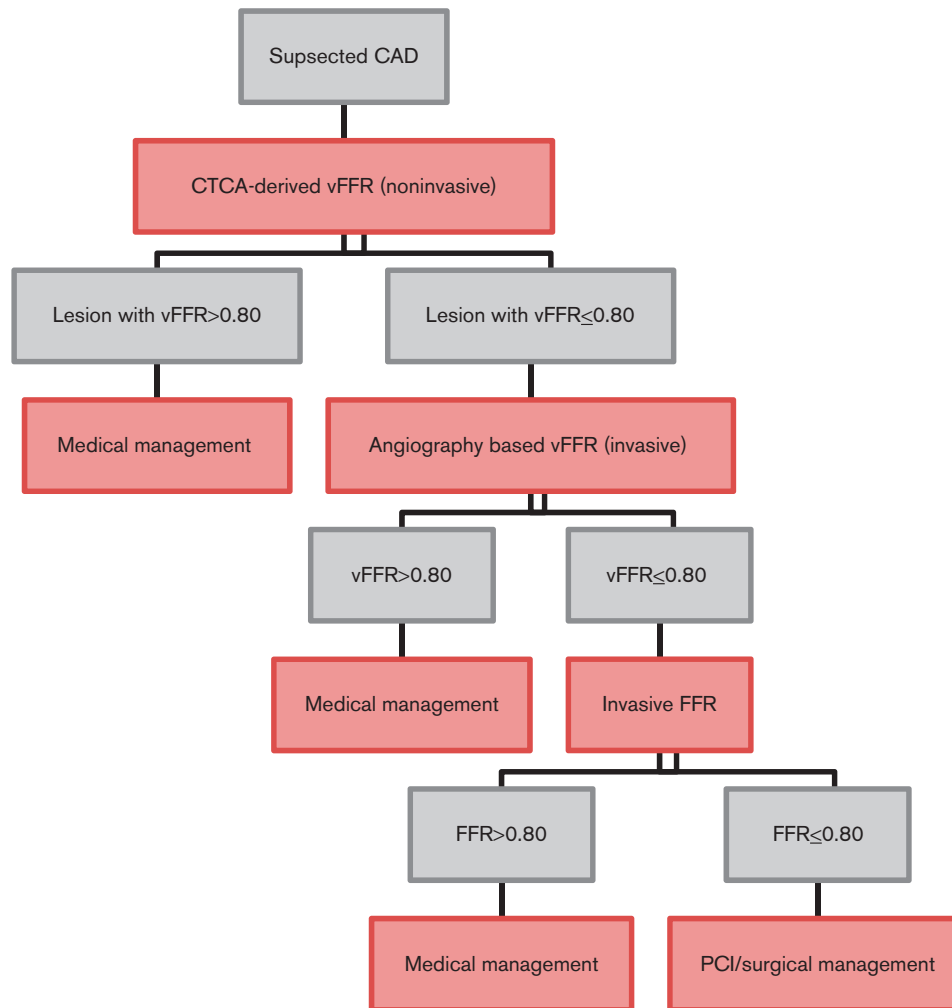## Future of virtual fractional flow reserve

The concept of vFFR, whether derived from CTCA or invasive angiography, is inherently attractive for several reasons. First, CTCA-derived vFFR is able to non-invasively identify physiologically significant stenoses with excellent accuracy, specificity, and high negative predictive value [65–67]. Second, whereas still invasive, angiography-based vFFR obviates the need for hyperaemia induction, expensive pressure wire catheters, and reduces the risk of procedural complications associated with invasive FFR [31,32,74]. These observations suggest a complementary, rather than competing, role for both methodologies in the clinical management of CAD

Fig. 3
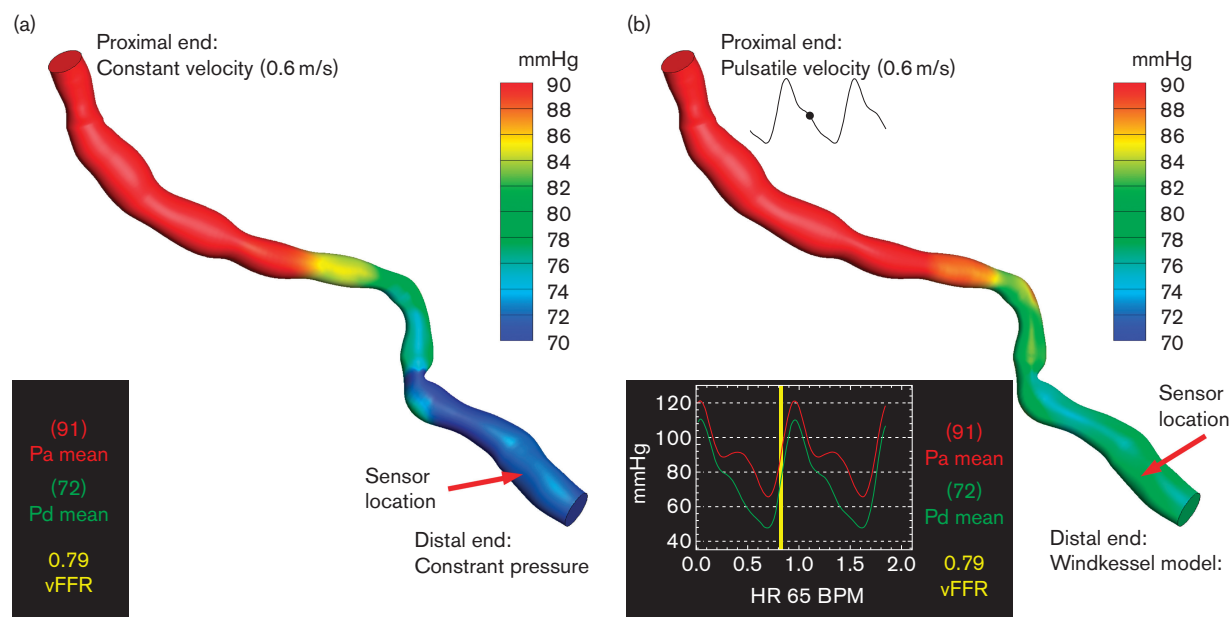
Virtual fractional flow reserve (vFFR) on case 0 with per cent diameter stenosis = 55 and invasive fractional flow reserve (FFR) = 0.80, vFFR = 0.79. Blood pressure levels across the stenosis are represented by the colour contours of mmHg. Distal pressure (Pd) was measured at the pressure sensor location identified from coronary angiography during invasive FFR (red arrows). Aortic pressure (Pa) was obtained at the proximal end of the artery. (a) Steady blood flow velocity and (b) pulsatile blood flow velocity. For pulsatile computational fluid dynamics study, the blood pressure levels are presented at the time-instant when the instantaneous blood flow velocity is the same as the steady blood flow velocity. That is, instantaneous blood flow velocity at 0.6 m/s. BPM, beats per min; HR, heart rate.

Fig. 4

Potential screening and treatment roles of virtual fractional flow reverse (vFFR) derived from coronary computed tomographic angiography and quantitative coronary angiography in the management of patients with suspected coronary artery disease (CAD). CTCA, coronary computed tomographic angiography; FFR, fractional flow reserve; PCI, percutaneous coronary intervention.

(see Fig. 4). The high sensitivity and negative predictive value of CTCA-derived vFFR may be useful in effectively ruling out physiologically significant lesions, thereby reducing the number of unnecessary referrals for invasive coronary angiography. Alternatively, in patients appropriately referred for invasive coronary angiography, vFFR may then be used instead of invasive FFR to further reduce procedural risk and cost.

Despite its daunting potential, the clinical application of vFFR remains elusive in its current state. In order to bridge the gap between vFFR and invasive FFR, two major challenges need to be addressed. The first challenge is an improvement to the overall workflow, both in terms of the execution time of the Navier–Stokes solver and the background skill-set required to perform a simulation. The second challenge is to improve patient specificity of the results both in terms of the geometric detail of the model and the imposition of boundary conditions.

To address the first major challenge a departure from standard Navier–Stokes solvers to specially tuned one-dimensional or 2D axisymmetric models, or Lattice Boltzmann methods may be required. With the former approach, a reduced order one-dimensional or 2D axisymmetric model would considerably reduce the size of the computational domain (and hence the amount of computation required to obtain a solution), but may still be able to capture the physics of the flow with sufficient accuracy to estimate the pressure difference. An additional benefit of such an approach would be the simplified mesh generation process, which would be orders of magnitude faster and could potentially be completely

automated, thereby removing the need for an engineer skilled in this field. With a Lattice Boltzmann method, again, the mesh generation procedure is simplified to the point of being trivial and the implicit parallelizability of the method means that 2D or 3D flow fields can be computed significantly faster on generic CPU-based supercomputing platforms or using graphics processing units [80].

Second, refinement in medical imaging data will also improve the accuracy, sensitivity and specificity of vFFR. Tight integration of coronary angiography and OCT (e.g. with coregistration) can lead to more accurate patient-specific coronary artery reconstructions [76], increased accuracy of vFFR simulations due to its high-fidelity and resolution, thereby providing better insight into the alteration of haemodynamics in the presence of stenoses.

In terms of addressing the issue of generic boundary conditions, use of the thrombolysis in myocardial infarction frame count to determine a patient-specific input for volumetric flow rate may be extended in an even more sophisticated manner to dynamically tune the boundary conditions. By solving an additional transport equation (describing the motion of the dye) with the standard Navier–Stokes equations, a synthetically generated concentration field could be generated. In this case, the observed and computed concentration fields could be used to pose vFFR as an optimization problem, dynamically tuning the boundary conditions until a misfit function describing the discrepancy between the observed and computed motion of the dye is minimized.

Ultimately, for this technology to be incorporated into routine clinical practice, medical image data processing and CFD simulations need to be automated [69] and simplified [81] such that patient-specific vFFR values can be obtained in an actionable time-frame. An automated process resulting in fast and highly accurate online vFFR would provide interventional cardiologists the optimum strategies for treatment of CAD, benefiting more patients and potentially cutting healthcare costs.

Conclusion
Anatomic and physiologic assessments of coronary stenoses remain the foundation of clinical cardiology. The standard techniques of 2D coronary angiography and invasive FFR measurements have rapidly given way to more advanced methodologies incorporating 3D quantitative angiography, coronary computed tomographic angiography, OCT and CFD simulations in calculating virtually derived FFR. In its current state, vFFR correlates moderately well and has many potential benefits over invasive FFR; however, several critical issues continue to hinder its wider clinical application. Higher image resolution and accuracy of 3D coronary artery models, more robust understanding and treatment of numerical boundary conditions, enhanced computational

time, and more streamlined workflows will help bring vFFR into mainstream clinical practice.

Conflicts of interest
There are no conflicts of interest.

References
1   Garrone P, Biondi-Zoccai G, Salvetti I, Sina N, Sheiban I, Stella PR, *et al.* Quantitative coronary angiography in the current era: principles and applications. *J Interv Cardiol* 2009; **22**:527–536.
2   Prati F, Di Vito L, Biondi-Zoccai G, Occhipinti M, La Manna A, Tamburino C, *et al.* Angiography alone versus angiography plus optical coherence tomography to guide decision-making during percutaneous coronary intervention: the Centro per la Lotta contro l'Infarto-Optimisation of Percutaneous Coronary Intervention (CLI-OPCI) study. *EuroIntervention* 2012; **8**:823–829.
3   Prati F, Regar E, Mintz GS, Arbustini E, Di Mario C, Jang I-K, *et al.* Expert review document on methodology, terminology, and clinical applications of optical coherence tomography: physical principles, methodology of image acquisition, and clinical application for assessment of coronary arteries and atherosclerosis. *Eur Heart J* 2010; **31**:401–415.
4   Tearney GJ, Regar E, Akasaka T, Adriaenssens T, Barlis P, Bezerra HG, *et al.* Consensus standards for acquisition, measurement, and reporting of intravascular optical coherence tomography studies: a report from the International Working Group for Intravascular Optical Coherence Tomography Standardization and Validation. *J Am Coll Cardiol* 2012; **59**:1058–1072.
5   Nakamura M. Angiography is the gold standard and objective evidence of myocardial ischemia is mandatory if lesion severity is questionable – indication of PCI for angiographically significant coronary artery stenosis without objective evidence of myocardial ischemia. *Circ J* 2011; **75**:204–210; discussion 217.
6   Marcus ML, Skorton DJ, Johnson MR, Collins SM, Harrison DG, Kerber RE. Visual estimates of percent diameter coronary stenosis: 'a battered gold standard'. *J Am Coll Cardiol* 1988; **11**:882–885.
7   Raphael MJ, Donaldson RM. A 'significant' stenosis: thirty years on. *Lancet* 1989; **1**:207–209.
8   DeRouen TA, Murray JA, Owen W. Variability in the analysis of coronary arteriograms. *Circulation* 1977; **55**:324–328.
9   Fisher LD, Judkins MP, Lesperance J, Cameron A, Swaye P, Ryan T, *et al.* Reproducibility of coronary arteriographic reading in the coronary artery surgery study (CASS). *Cathet Cardiovasc Diagn* 1982; **8**:565–575.
10   Desmet W, Willems J, Van Lierde J, Piessens J. Discrepancy between visual estimation and computer-assisted measurement of lesion severity before and after coronary angioplasty. *Cathet Cardiovasc Diagn* 1994; **31**:192–198.
11   Tu S, Barbato E, Köszegi Z, Yang J, Sun Z, Holm NR, *et al.* Fractional flow reserve calculation from 3-dimensional quantitative coronary angiography and TIMI frame count: a fast computer model to quantify the functional significance of moderately obstructed coronary arteries. *JACC Cardiovasc Interv* 2014; **7**:768–777.
12   Nallamothu BK, Spertus JA, Lansky AJ, Cohen DJ, Jones PG, Kureshi F, *et al.* Comparison of clinical interpretation with visual assessment and quantitative coronary angiography in patients undergoing percutaneous coronary intervention in contemporary practice: the Assessing Angiography (A2) project. *Circulation* 2013; **127**:1793–1800.
13   Leape LL, Park RE, Bashore TM, Harrison JK, Davidson CJ, Brook RH. Effect of variability in the interpretation of coronary angiograms on the

appropriateness of use of coronary revascularization procedures. *Am Heart J* 2000; **139**:106–113.

14 Goldberg RK, Kleiman NS, Minor ST, Abukhalil J, Raizner AE. Comparison of quantitative coronary angiography to visual estimates of lesion severity pre and post PTCA. *Am Heart J* 1990; **119**:178–184.

15 Mancini GB. Quantitative coronary arteriographic methods in the interventional catheterization laboratory: an update and perspective. *J Am Coll Cardiol* 1991; **17**:23B–33B.

16 Foley DP, Escaned J, Strauss BH, Mario C, Haase J, Keane D, *et al.* Quantitative coronary angiography (QCA) in interventional cardiology: clinical application of QCA measurements. *Prog Cardiovasc Dis* 1994; **36**:363–384.

17 Thomas AC, Davies MJ, Dilly S, Dilly N, Franc F. Potential errors in the estimation of coronary arterial stenosis from clinical arteriography with reference to the shape of the coronary arterial lumen. *Br Heart J* 1986; **55**:129–139.

18 Dvir D, Marom H, Guetta V, Kornowski R. Three-dimensional coronary reconstruction from routine single-plane coronary angiograms: in vivo quantitative validation. *Int J Cardiovasc Intervent* 2005; **7**:141–145.

19 Bourantas CV, Tweddel AC, Papafaklis MI, Karvelis PS, Fotiadis DI, Katsouras CS, *et al.* Comparison of quantitative coronary angiography with intracoronary ultrasound. Can quantitative coronary angiography accurately estimate the severity of a luminal stenosis? *Angiology* 2008; **60**:169–179.

20 Tu S, Xu L, Ligthart J, Xu B, Witberg K, Sun Z, *et al.* In vivo comparison of arterial lumen dimensions assessed by co-registered three-dimensional (3D) quantitative coronary angiography, intravascular ultrasound and optical coherence tomography. *Int J Cardiovasc Imaging* 2012; **28**:1315–1327.

21 Tu S, Jing J, Holm NR, Onsea K, Zhang T, Adriaenssens T, *et al.* In vivo assessment of bifurcation optimal viewing angles and bifurcation angles by three-dimensional (3D) quantitative coronary angiography. *Int J Cardiovasc Imaging* 2012; **28**:1617–1625.

22 Gonzalo N, Garcia-Garcia HM, Regar E, Barlis P, Wentzel J, Onuma Y, *et al.* In vivo assessment of high-risk coronary plaques at bifurcations with combined intravascular ultrasound and optical coherence tomography. *JACC Cardiovasc Imaging* 2009; **2**:473–482.

23 Barlis P, Dimopoulos K, Tanigawa J, Dzielicka E, Ferrante G, Del Furia F, *et al.* Quantitative analysis of intracoronary optical coherence tomography measurements of stent strut apposition and tissue coverage. *Int J Cardiol* 2010; **141**:151–156.

24 Takagi A, Tsurumi Y, Ishii Y, Suzuki K, Kawana M, Kasanuki H. Clinical potential of intravascular ultrasound for physiological assessment of coronary stenosis: relationship between quantitative ultrasound tomography and pressure-derived fractional flow reserve. *Circulation* 1999; **100**:250–255.

25 Briguori C, Anzuini A, Airoldi F, Gimelli G, Nishida T, Adamian M, *et al.* Intravascular ultrasound criteria for the assessment of the functional significance of intermediate coronary artery stenoses and comparison with fractional flow reserve. *Am J Cardiol* 2001; **87**:136–141.

26 Kang S-J, Lee J-Y, Ahn J-M, Mintz GS, Kim W-J, Park D-W, *et al.* Validation of intravascular ultrasound-derived parameters with fractional flow reserve for assessment of coronary stenosis severity. *Circ Cardiovasc Interv* 2011; **4**:65–71.

27 Gonzalo N, Gonzalo N, Escaned J, Alfonso F, Nolte C, Rodriguez V, *et al.* Morphometric assessment of coronary stenosis relevance with optical coherence tomography: a comparison with fractional flow reserve and intravascular ultrasound. *J Am Coll Cardiol* 2012; **59**:1080–1089.

28 Shiono Y, Kitabata H, Kubo T, Masuno T, Ohta S, Ozaki Y, *et al.* Optical coherence tomography-derived anatomical criteria for functionally significant coronary stenosis assessed by fractional flow reserve. *Circ J* 2012; **76**:2218–2225.

29 Zafar H, Ullah I, Dinneen K, Matiullah S, Hanley A, Leahy MJ, *et al.* Evaluation of hemodynamically severe coronary stenosis as determined by fractional flow reserve with frequency domain optical coherence tomography measured anatomical parameters. *J Cardiol* 2014; **64**:19–24.

30 Alfonso F, Macaya C, Goicolea J, Hernandez R, Bañuelos C, Iñiguez A, *et al.* Angiographic changes (Dotter effect) produced by intravascular ultrasound imaging before coronary angioplasty. *Am Heart J* 1994; **128**:244–251.

31 Elgendy IY, Conti CR, Bavry AA. Fractional flow reserve: an updated review. *Clin Cardiol* 2014; **37**:371–380.

32 Koo B-K. The present and future of fractional flow reserve. *Circ J* 2014; **78**:1048–1054.

33 Rassi AN, O'Dea JA, Jia H, Seto AH, Jang I-K. Nonangiographic assessment of coronary artery disease: a practical approach to optical coherence tomography and fractional flow reserve. *Coron Artery Dis* 2014; **25**:608–618.

34 Ullah M, Majumder AAS. Fractional flow reserve – a review. *Cardiovasc J* 2013; **5**:190–200.

35 Pijls NHJ, Fearon WF, Tonino PAL, Siebert U, Ikeno F, Bornschein B, *et al.* Fractional flow reserve versus angiography for guiding percutaneous coronary intervention in patients with multivessel coronary artery disease: 2-year follow-up of the FAME (Fractional Flow Reserve Versus Angiography for Multivessel Evaluation) study. *J Am Coll Cardiol* 2010; **56**:177–184.

36 Pijls NHJ, van Schaardenburgh P, Manoharan G, Boersma E, Bech J-W, van't Veer M, *et al.* Percutaneous coronary intervention of functionally nonsignificant stenosis: 5-year follow-up of the DEFER study. *J Am Coll Cardiol* 2007; **49**:2105–2111.

37 Van Belle E, Rioufol G, Pouillot C, Cuisset T, Bougrini K, Teiger E, *et al.* Outcome impact of coronary revascularization strategy reclassification with fractional flow reserve at time of diagnostic angiography: insights from a large French multicenter fractional flow reserve registry. *Circulation* 2014; **129**:173–185.

38 Li J, Elrashidi MY, Flammer AJ, Lennon RJ, Bell MR, Holmes DR, *et al.* Long-term outcomes of fractional flow reserve-guided vs. angiography-guided percutaneous coronary intervention in contemporary practice. *Eur Heart J* 2013; **34**:1375–1383.

39 Park S-J, Ahn J-M, Park G-M, Cho Y-R, Lee J-Y, Kim W-J, *et al.* Trends in the outcomes of percutaneous coronary intervention with the routine incorporation of fractional flow reserve in real practice. *Eur Heart J* 2013; **34**:3353–3361.

40 Hoole SP, Seddon MD, Poulter RS, Starovoytov A, Wood DA, Saw J. Development and validation of the fractional flow reserve (FFR) angiographic scoring tool (FAST) to improve the angiographic grading and selection of intermediate lesions that require FFR assessment. *Coron Artery Dis* 2012; **23**:45–50.

41 Courtis J, Rodés-Cabau J, Larose E, Déry J-P, Nguyen CM, Proulx G, *et al.* Comparison of medical treatment and coronary revascularization in patients with moderate coronary lesions and borderline fractional flow reserve measurements. *Catheter Cardiovasc Interv* 2008; **71**:541–548.

42 Lindstaedt M, Halilcavusogullari Y, Yazar A, Holland-Letz T, Bojara W, Mügge A, *et al.* Clinical outcome following conservative vs revascularization therapy in patients with stable coronary artery disease and borderline fractional flow reserve measurements. *Clin Cardiol* 2010; **33**:77–83.

43 Van de Hoef TP, Nolte F, Echavarrĺa-Pinto M, van Lavieren MA, Damman P, Chamuleau SAJ, *et al.* Impact of hyperaemic microvascular resistance on fractional flow reserve measurements in patients with stable coronary artery disease: insights from combined stenosis and microvascular resistance assessment. *Heart* 2014; **100**:951–959.

44 Fearon WF, Bornschein B, Tonino PAL, Gothe RM, BD Bruyne, Pijls NHJ, Siebert U. Fractional Flow Reserve Versus Angiography for Multivessel Evaluation (FAME) Study Investigators. Economic evaluation of fractional flow reserve-guided percutaneous coronary intervention in patients with multivessel disease. *Circulation* 2010; **122**:2545–2550.

45 Fearon WF. Percutaneous coronary intervention should be guided by fractional flow reserve measurement. *Circulation* 2014; **129**:1860–1870.

46 Wijns W, Kolh P, Danchin N, Di Mario C, Falk V, Folliguet T, *et al.* Guidelines on myocardial revascularization. *Eur Heart J* 2010; **31**:2501–2555.

47 Kushner FG, Hand M, Smith SC, King SB, Anderson JL, Antman EM, *et al.* 2009 focused updates: ACC/AHA guidelines for the management of patients with ST-elevation myocardial infarction (updating the 2004 guideline and 2007 focused update) and ACC/AHA/SCAI guidelines on percutaneous coronary intervention (updating the 2005 guideline and 2007 focused update) a report of the American College of Cardiology Foundation/American Heart Association Task Force on Practice Guidelines. *J Am Coll Cardiol* 2009; **54**:2205–2241.

48 Schelbert HR. FFR and coronary flow reserve: friends or foes? *JACC Cardiovasc Imaging* 2012; **5**:203–206.

49 Gould KL, Lipscomb K, Hamilton GW. Physiologic basis for assessing critical coronary stenosis. *Am J Cardiol* 1974; **33**:87–94.

50 Meimoun P, Benali T, Sayah S, Luycx-Bore A, Boulanger J, Zemir H, *et al.* Evaluation of left anterior descending coronary artery stenosis of intermediate severity using transthoracic coronary flow reserve and dobutamine stress echocardiography. *J Am Soc Echocardiogr* 2005; **18**:1233–1240.

51 Okayama H, Sumimoto T, Hiasa G, Nishimura K, Morioka N, Yamamoto K, *et al.* Assessment of intermediate stenosis in the left anterior descending coronary artery with contrast-enhanced transthoracic Doppler echocardiography. *Coron Artery Dis* 2003; **14**:247–254.

52 Meimoun P, Benali T, Elmkies F, Sayah S, Luycx-Bore A, Doutrelan L, *et al.* Prognostic value of transthoracic coronary flow reserve in medically treated patients with proximal left anterior descending artery stenosis of intermediate severity. *Eur J Echocardiogr* 2009; **10**:127–132.

53 D'Andrea A, Severino S, Mita C, Riegler L, Cocchia R, Gravino R, *et al.* Clinical outcome in patients with intermediate stenosis of left anterior

descending coronary artery after deferral of revascularization on the basis of noninvasive coronary flow reserve measurement. *Echocardiography* 2009; **26**:431–440.

54   Serruys PW. The great iFR vs. FFR debate: why sometimes 'the wait and see approach' is the best tactic as the best pragmatic solution will always emerge and become established. *EuroIntervention* 2013; **9**:11–13.

55   Young DF, Cholvin NR, Roth AC. Pressure drop across artificially induced stenoses in the femoral arteries of dogs. *Circ Res* 1975; **36**:735–743.

56   Young DF, Tsai FY. Flow characteristics in models of arterial stenoses: II. Unsteady flow. *J Biomech* 1973; **6**:547–559.

57   Gould KL, Kirkeeide RL, Buchi M. Coronary flow reserve as a physiologic measure of stenosis severity. *J Am Coll Cardiol* 1990; **15**:459–474.

58   Di Mario C, Gil R, de Feyter PJ, Schuurbiers JC, Serruys PW. Utilization of translesional hemodynamics: comparison of pressure and flow methods in stenosis assessment in patients with coronary artery disease. *Cathet Cardiovasc Diagn* 1996; **38**:189–201.

59   Meimoun P, Sayah S, Luycx-Bore A, Boulanger J, Elmkies F, Benali T, et al. Comparison between non-invasive coronary flow reserve and fractional flow reserve to assess the functional significance of left anterior descending artery stenosis of intermediate severity. *J Am Soc Echocardiogr* 2011; **24**:374–381.

60   Johnson NP, Kirkeeide RL, Gould KL. Is discordance of coronary flow reserve and fractional flow reserve due to methodology or clinically relevant coronary pathophysiology? *JACC Cardiovasc Imaging* 2012; **5**:193–202.

61   Gould KL, Johnson NP, Bateman TM, Beanlands RS, Bengel FM, Bober R, et al. Anatomic versus physiologic assessment of coronary artery disease. Role of coronary flow reserve, fractional flow reserve, and positron emission tomography imaging in revascularization decision-making. *J Am Coll Cardiol* 2013; **62**:1639–1653.

62   Petraco R, Sen S, Nijjer S, Echavarria-Pinto M, Escaned J, Francis DP, et al. Fractional flow reserve-guided revascularization: practical implications of a diagnostic gray zone and measurement variability on clinical decisions. *JACC Cardiovasc Interv* 2013; **6**:222–225.

63   Kern MJ. Reconciling poststenotic pressure with hyperemic flow: comparing coronary flow reserve, instantaneous wave-free ratio, and fractional flow reserve. *Circ Cardiovasc Interv* 2014; **7**:432–434.

64   Seto AH, Tehrani DM, Bharmal MI, Kern MJ. Variations of coronary hemodynamic responses to intravenous adenosine infusion: Implications for fractional flow reserve measurements. *Catheter Cardiovasc Interv* 2014; **84**:416–425.

65   Petraco R, van de Hoef TP, Nijjer S, Sen S, van La vieren MA, Foale RA, et al. Baseline instantaneous wave-free ratio as a pressure-only estimation of underlying coronary flow reserve: results of the JUSTIFY-CFR study (Joined Coronary Pressure and Flow Analysis to Determine Diagnostic Characteristics of Basal and Hyperemic Indicesof Functional Lesion Severity-Coronary Flow Reserve). *Circ Cardiovasc Interv* 2014; **7**:492–502.

66   Pijls NHJ, Tonino PAL. The crux of maximum hyperemia: the last remaining barrier for routine use of fractional flow reserve. *JACC Cardiovasc Interv* 2011; **4**:1093–1095.

67   Koo B-K, Erglis A, Doh J-H, Daniels DV, Jegere S, Kim H-S, et al. Diagnosis of ischemia-causing coronary stenoses by noninvasive fractional flow reserve computed from coronary computed tomographic angiograms. Results from the prospective multicenter DISCOVER-FLOW (Diagnosis of Ischemia-Causing Stenoses Obtained Via Noni). *J Am Coll Cardiol* 2011; **58**:1989–1997.

68   Min JK, Berman DS, Budoff MJ, Jaffer FA, Leipsic J, Leon MB, et al. Rationale and design of the DeFACTO (Determination of Fractional Flow Reserve by Anatomic Computed Tomographic AngiOgraphy) study. *J Cardiovasc Comput Tomogr* 2011; **5**:301–309.

69   Nørgaard BL, Leipsic J, Gaur S, Seneviratne S, Ko BS, Ito H, et al. Diagnostic performance of noninvasive fractional flow reserve derived from coronary computed tomography angiography in suspected coronary artery disease: the NXT trial (Analysis of Coronary Blood Flow Using CT Angiography: Next Steps). *J Am Coll Cardiol* 2014; **63**:1145–1155.

70   Morris PD, Ryan D, Morton AC, Lycett R, Lawford PV, Hose DR, et al. Virtual fractional flow reserve from coronary angiography: modeling the significance of coronary lesions: results from the VIRTU-1 (VIRTUal Fractional Flow Reserve From Coronary Angiography) study. *JACC Cardiovasc Interv* 2013; **6**:149–157.

71   Papafaklis MI, Muramatsu T, Ishibashi Y, Lakkas LS, Nakatani S, Bourantas CV, et al. Fast virtual functional assessment of intermediate coronary lesions using routine angiographic data and blood flow simulation in humans: comparison with pressure wire – fractional flow reserve. *EuroIntervention* 2014; **10**:574–583.

72   Kim HJ, Vignon-Clementel IE, Coogan JS, Figueroa CA, Jansen KE, Taylor CA. Patient-specific modeling of blood flow and pressure in human coronary arteries. *Ann Biomed Eng* 2010; **38**:3195–3209.

73   Taylor CA, Fonte TA, Min JK. Computational fluid dynamics applied to cardiac computed tomography for noninvasive quantification of fractional flow reserve: scientific basis. *J Am Coll Cardiol* 2013; **61**:2233–2241.

74   Foin N, Petraco R, Sen S, Nijjer S, Davies JE. Assessment of lesion functional significance with virtual FFR – are we going with the flow? *EuroIntervention* 2014; **10**:535–538.

75   Gaur S, Bezerra HG, Lassen JF, Christiansen EH, Tanaka K, Jensen JM, et al. Fractional flow reserve derived from coronary CT angiography: variation of repeated analyses. *J Cardiovasc Comput Tomogr* 2014; **8**:307–314.

76   Kousera CA, Nijjer S, Torii R, Petraco R, Sen S, Foin N, et al. Patient-specific coronary stenoses can be modeled using a combination of OCT and flow velocities to accurately predict hyperemic pressure gradients. *IEEE Trans Biomed Eng* 2014; **61**:1902–1913.

77   Sen S, Escaned J, Malik IS, Mikhail GW, Foale RA, Mila R, et al. Development and validation of a new adenosine-independent index of stenosis severity from coronary wave-intensity analysis: results of the ADVISE (ADenosine Vasodilator Independent Stenosis Evaluation) study. *J Am Coll Cardiol* 2012; **59**:1392–1402.

78   Malek AM, Alper SL, Izumo S. Hemodynamic shear stress and its role in atherosclerosis. *J Am Med Assoc* 1999; **282**:2035–2042.

79   Blackburn HM, Sherwin SJ. Instability modes and transition of pulsatile stenotic flow: pulse-period dependence. *J Fluid Mech* 2007; **573**:57.

80   Nita C, Itu LM, Suciu C. GPU accelerated blood flow computation using the Lattice Boltzmann Method. 2013 IEEE High Performance Extreme Computing Conference (HPEC); 10–12 September 2013; Waltham, MA. pp. 1–6.

81   Schrauwen JTC, Wentzel JJ, van der Steen AFW, Gijsen FJH. Geometry-based pressure drop prediction in mildly diseased human coronary arteries. *J Biomech* 2014; **47**:1810–1815.